ADVANCED MATERIALS

Supporting Information

for *Adv. Mater.*, DOI: 10.1002/adma.201902364

Depth-Resolved Modulation of Metal–Oxygen Hybridization and Orbital Polarization across Correlated Oxide Interfaces

*Paul C. Rogge, Padraic Shafer, Gilberto Fabbris, Wen Hu, Elke Arenholz, Evguenia Karapetrova, Mark P. M. Dean, Robert J. Green, and Steven J. May**

Supporting Information

Depth-Resolved Modulation of Metal–Oxygen Hybridization and Orbital Polarization across Correlated Oxide Interfaces

*Paul C. Rogge, Padraic Shafer, Gilberto Fabbris, Wen Hu, Elke Arenholz, Evguenia Karapetrova, Mark P. M. Dean, Robert J. Green, and Steven J. May**

Superlattice Strain State

The strain state of the superlattice was probed using hard x-ray diffraction. A reciprocal space map of the substrate and superlattice 103 Bragg peaks is shown in Figure S1(a). The $LaAlO_3$ 103 peak has strong intensity that spans a range of q_x values due to the twinned nature of the $LaAlO_3$ substrate. Intensity centered at $q_x \sim 1.62$ Å^{-1}, $q_z \sim 4.94$ Å^{-1} is attributed to the superlattice. The shift to lower q_x values relative to the $LaAlO_3$ substrate confirms that the superlattice is relaxed from the substrate. The approximate *c*-axis parameters of $SrFeO_3$ and $CaFeO_3$ were extracted from X-ray diffraction measured across the $LaAlO_3$ 002 Bragg peak, shown in Figure S1(b), which exhibits satellite peaks associated with the film's superstructure. The hard x-ray spot size was 3 mm x 0.5 mm, and the $LaAlO_3$ 002 peak is broadened due to the twins, which broaden the superstructure features of the film as well. The diffraction intensity was simulated using GenX,[S1] where the previously determined layer thicknesses obtained from the 800 eV off-resonance reflectivity analysis shown in the main manuscript were used. The simulated intensity shown in Figure S1(b) is for perfect crystallinity with no interfacial roughness or intermixing, whereas smearing the intensity with a Gaussian function (FWHM = 0.006 reciprocal lattice units) in order to model the broadening due to the substrate twins results in the simulated intensity shown in Figure S1(c). As seen in Figure S1(b) and S1(c), good agreement is achieved for a $SrFeO_3$ *c*-axis parameter of 3.85 Å and a $CaFeO_3$ *c*-axis parameter of 3.73 Å. Given the bulk *c*-axis parameters of 3.85 Å for $SrFeO_3$ and 3.77 Å for $CaFeO_3$,[S2,S3] this suggests that $SrFeO_3$ is relaxed but that $CaFeO_3$ is under tensile strain (1.9%). From previous results of strained $CaFeO_3$ films, this obtained $CaFeO_3$ *c*-axis parameter correlates with an in-plane spacing of that equal to the bulk $SrFeO_3$ spacing.[S4] This suggests that the thicker $SrFeO_3$ layers are relaxed from the substrate but the thinner $CaFeO_3$ layers are strained to the $SrFeO_3$ layers. Considering the relaxed superlattice as a simple parallel-plate system, the average in-plane lattice parameter would be equal to an average of the bulk lattice parameters weighted by their respective layer thicknesses, which would give ~3.83 Å, in which case $SrFeO_3$ would be under small compressive strain (-0.5%) and $CaFeO_3$ under moderate tensile strain (+1.6%).

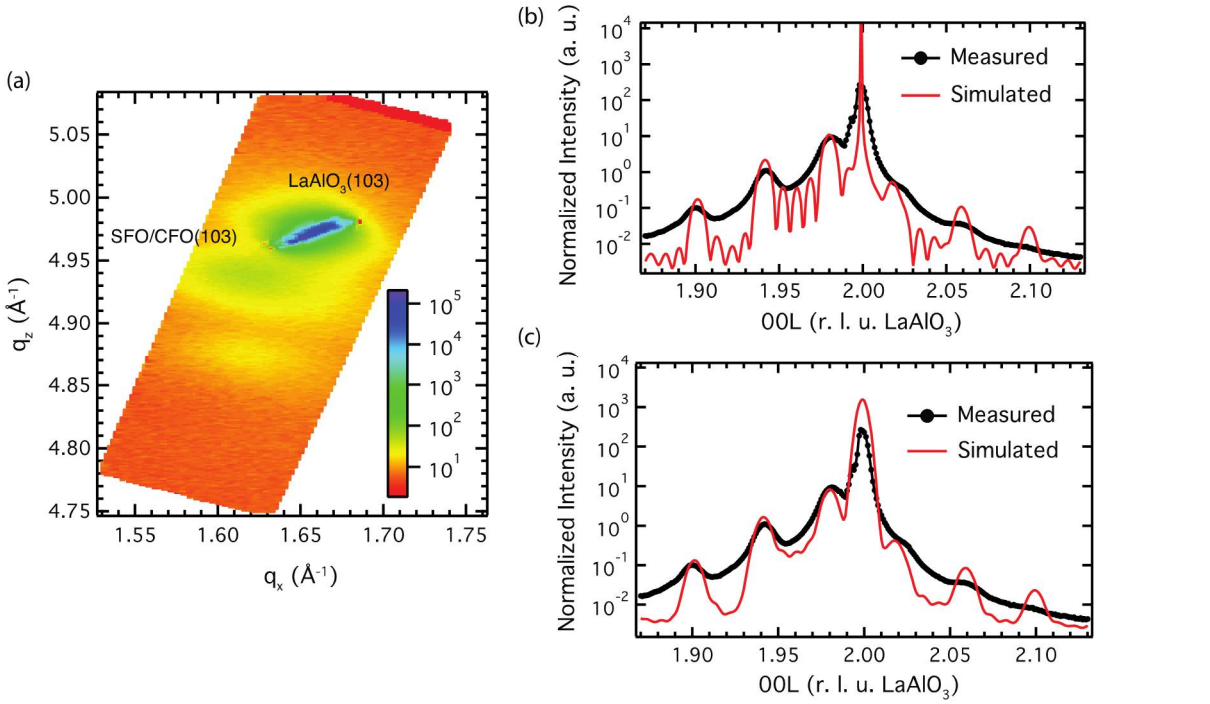

Figure S1. Hard x-ray diffraction of the $[(SrFeO_3)_{20}/(CaFeO_3)_5]$x4 superlattice with a 22 unit-cell-thick $SrFeO_3$ capping layer. (a) Reciprocal space map around the substrate and superlattice 103 Bragg peaks measured with 8.047 keV photons (Cu K_α). (b) Diffraction intensity obtained by a symmetric scan across the $LaAlO_3$ 002 Bragg peak with 16.000 keV photons. The simulated 002 diffraction intensity is shown for $SrFeO_3$ with c = 3.85 Å and $CaFeO_3$ with c = 3.73 Å. (c) Smoothing the simulated 002 intensity with a Gaussian (FWHM = 0.006 r.l.u.) to account for the substrate twin-induced broadening improves the agreement with measured.

Oxygen Prepeak Optical Parameters

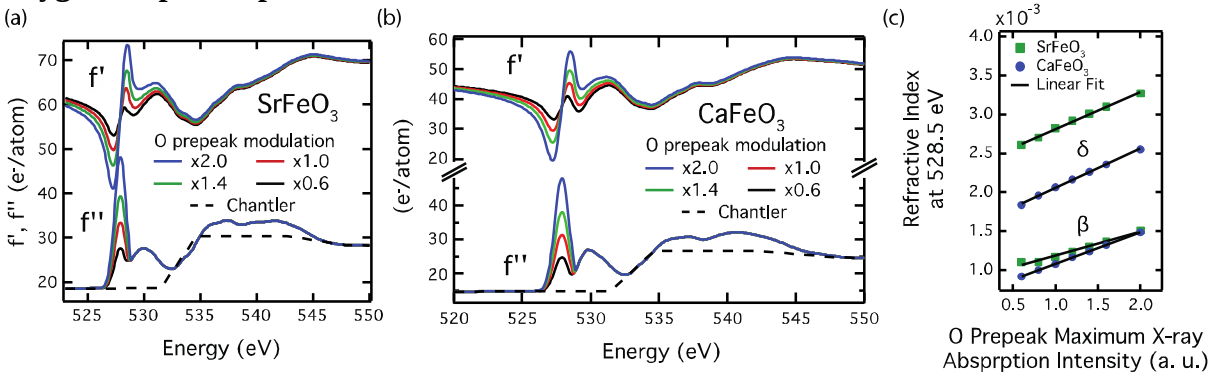

Figure S2. (a) The real (*f'*) and imaginary (*f''*) part of the resonant scattering factors for $SrFeO_3$ and (b) $CaFeO_3$ across the O *K* edge based on total electron yield (TEY) x-ray absorption measurements. Total fluorescence yield (TFY) spectra cannot be used due to substrate contributions to the measured O *K* edge. To simulate reflectivity from layers with different ligand hole densities, the intensity of the *f''* prepeak feature was modified by fitting a Gaussian curve to the prepeak feature in the original x-ray absorption spectrum. This Gaussian peak was then increased or decreased in intensity and then recombined with the measured x-ray absorption data outside the prepeak region. Because measuring x-ray absorption by the surface-sensitive TEY technique results in a suppressed prepeak intensity due to slight oxygen loss at the surface, the *f''* spectra that has a prepeak intensity approximately equal to the most intense feature at higher O *K* edge energies is set as the

baseline spectrum (labeled "x1.0"). This relative prepeak intensity to the main O *K* edge is more representative of bulk ferrates ($SrFeO_3$ and $CaFeO_3$).[S5] The dispersive part, *f'*, was computed via Kramers-Kronig conversion for each modified *f''* spectra. (c) The complex refractive index at 528.5 eV for $SrFeO_3$ and $CaFeO_3$ exhibits a linear relationship with the maximum prepeak intensity, which was used to constrain the fitting process of the prepeak reflectivity.

Fe Resonant Optical Parameters

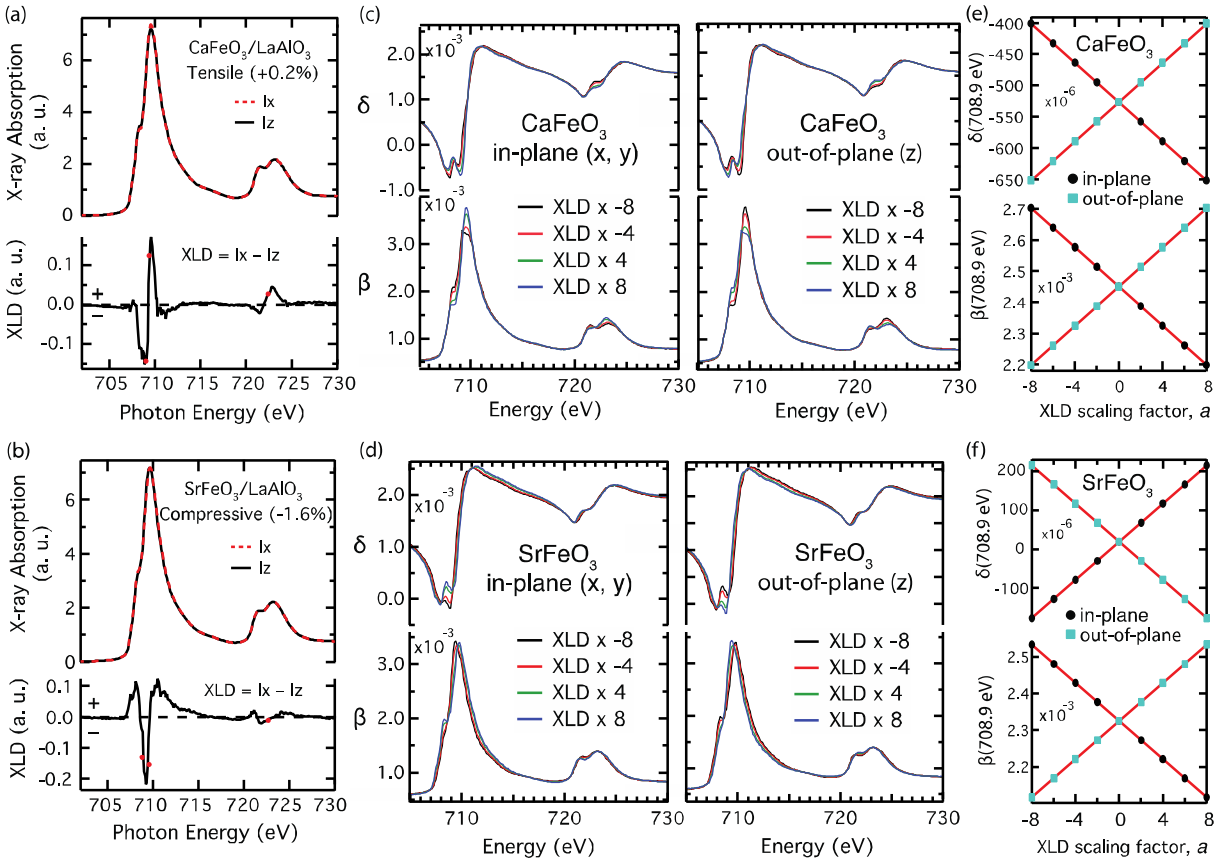

Figure S3. (a) Experimentally measured polarization-dependent x-ray absorption across the Fe *L* edge of a monolithic film of $CaFeO_3/LaAlO_3(001)$ and (b) $SrFeO_3/LaAlO_3(001)$. The x-ray linear dichroism (XLD) spectrum, $(I_x - I_z)$, is also shown, where the red circles denote the energies at which the Fe resonant reflectivity was measured. I_x (I_z) is the x-ray absorption intensity measured with photons polarized in-plane (out-of-plane) relative to the film surface. (c) Anisotropic refractive index ($N = 1 - \delta + i\beta$) as derived from experimentally measured polarization-dependent x-ray absorption of the monolithic film of $SrFeO_3/LaAlO_3(001)$ and (d) $CaFeO_3/LaAlO_3(001)$. To model different orbital occupations in $SrFeO_3$ and $CaFeO_3$, the XLD was multiplied by a given factor, *a*, and β was recomputed for both in-plane and out-of-plane polarizations, followed by determining δ via Kramers-Kronig conversion. (e)-(f) The extracted values of δ and β at 708.9 eV as a function of the XLD scaling factor, *a*, exhibit a linear trend, which was used to enable the reflectivity simulation software to vary the magnitude of the XLD in order to determine the best fit with the measured asymmetry at 708.9 eV.

Additional Fe Resonant Reflectivity Simulations

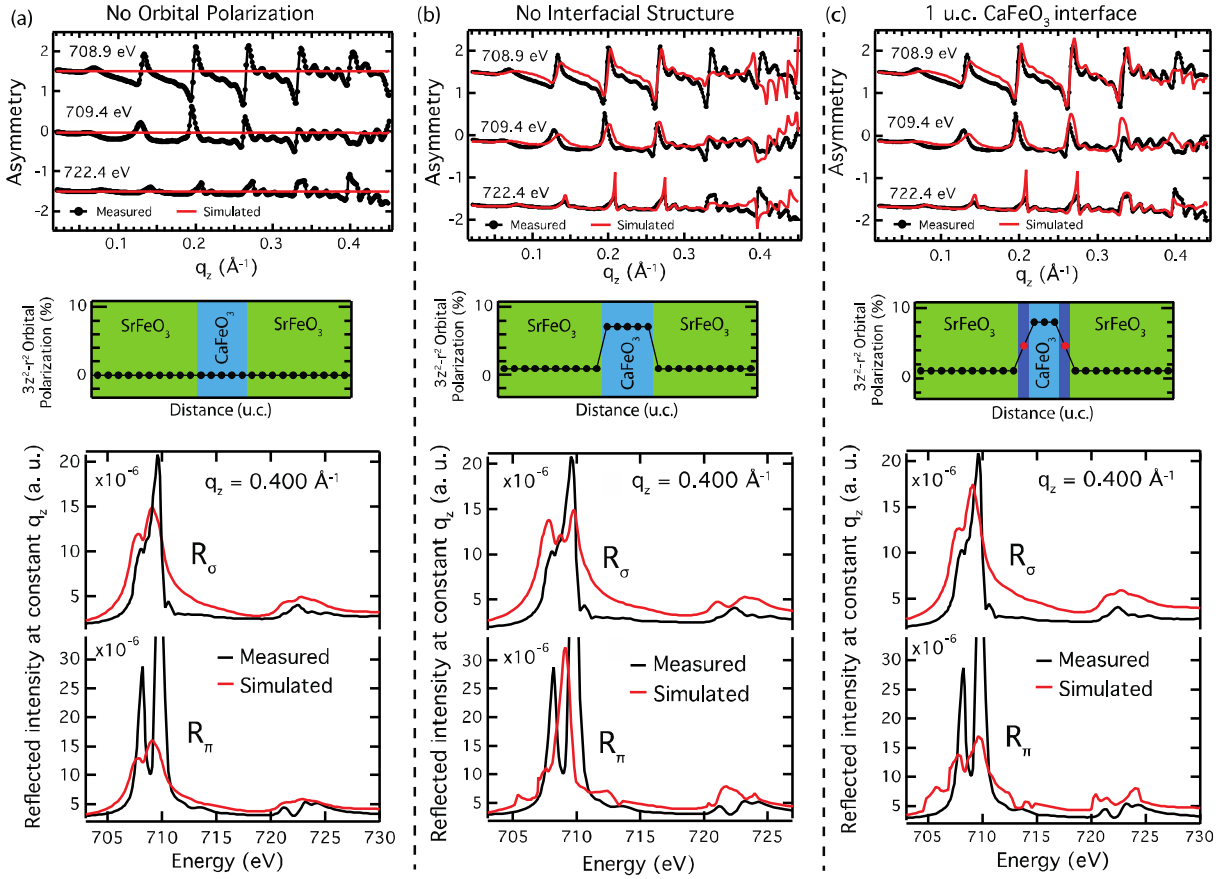

Figure S4. Evaluation of the Fe *L* edge resonant reflectivity with different layer orbital polarizations for three scenarios. Each scenario includes the measured and simulated reflected intensity asymmetry, $(R_\sigma - R_\pi)/(R_\sigma - R_\pi)$, a plot of the orbital polarization across the $SrFeO_3/CaFeO_3$ interface used to obtain each simulation, and the polarization-dependent reflected intensity at $q_{z,006} = 0.400$ Å^{-1} as a function of photon energy, which is sensitive to the interface between $CaFeO_3$ and $SrFeO_3$. (a) For no orbital polarization in either $SrFeO_3$ or $CaFeO_3$ (left), the asymmetry exhibits no features and moderate agreement is obtained for the constant q_z energy scan. (b) The obtained best fit with no interfacial regions occurs for a 1% $d_{3z^2-r^2}$ polarization in $SrFeO_3$ and a 7% $d_{3z^2-r^2}$ polarization in $CaFeO_3$. The simulated reflectivity exhibits moderate agreement for the asymmetry, but the constant q_z energy scan exhibits poor agreement with the experimental spectra, particularly on the π channel as well as at the Fe L_3 peak between 720-725 eV for both channels. (c) With the 1 unit-cell-thick $CaFeO_3$ interfacial structure, the best fit is obtained with a 1% $d_{3z^2-r^2}$ polarization in $SrFeO_3$ and a 8% $d_{3z^2-r^2}$ polarization in $CaFeO_3$ that is reduced to 4% $d_{3z^2-r^2}$ polarization in the interfacial layers, where the agreement between experiment and simulation for the asymmetry notably improves for $q_z > 0.3$ Å^{-1}, and the constant q_z scan shows improved agreement on the σ and π channels, particularly at the Fe L_2 peak.

Multiplet Ligand Field Calculations

We employed a standard multiplet ligand field theory model using the code *Quanty*, which computes the eigenstates and spectra using exact diagonalization. The model includes the Fe 3*d* shell, a ligand shell comprised of *d*-symmetry linear combinations of oxygen 2*p* orbitals, and the Fe core 2*p* shell. Parameters of the model include the local Fe Coulomb and exchange integrals (F^k_{dd}, F^k_{pd}, and G^k_{pd}), for which we use Hartree-Fock determined values[S6] that are

subsequently rescaled to account for atomic as well as solid state corrections using inter- and intra-shell rescaling factors κ_{dd} and κ_{pd}, respectively. We also include the Fe atomic 3*d* and 2*p* spin orbit interaction (66 meV and 8.199 eV, respectively). We further include the octahedral crystal field splitting 10*Dq*, the charge transfer energy Δ as well as the monopole parts of the valence-valence and core-valence Coulomb interactions (U_{dd} = 6 eV and U_{pd} = 8 eV, respectively). Finally, hybridization between the Fe 3*d* and ligand orbitals is included via O_h symmetry hopping integrals V_{e_g} and $V_{t_{2g}}$ ($\equiv 0.58V_{e_g}$),[S7] and in the XAS final state the hopping integrals are rescaled by V_f to account for orbital contraction due to the core hole. These parameters were optimized previously by comparing the calculated x-ray absorption spectrum with experiment[S4] and yielded 10*Dq* = 0.5 eV, V_{e_g} = 2.80 eV, V_f = 0.80, κ_{dd} = 0.65, κ_{pd} = 0.80, and Δ = -2.0 eV.

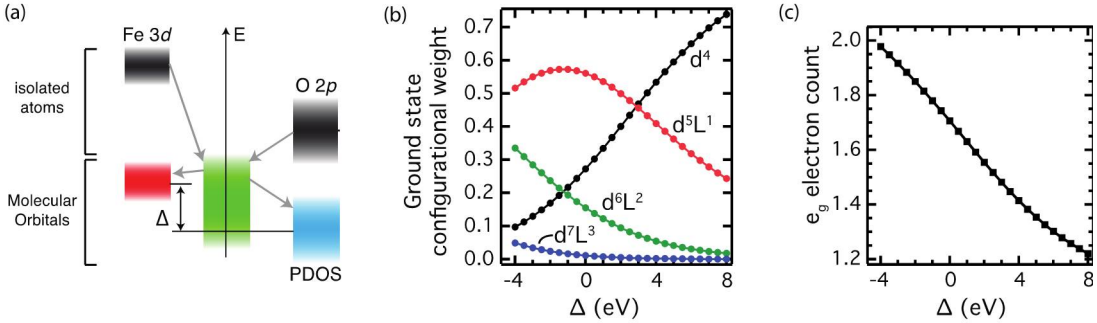

Figure S5. (a) Illustration of the energy alignment of the Fe 3*d* and O 2*p* partial density of states (PDOS) after isolated atoms hybridize, where the charge transfer energy, Δ, is the energy difference between the PDOS center of masses; the case for Δ > 0 is illustrated. (b) Configurational weight to the $CaFeO_3$ ground state as a function of the charge transfer energy. (c) The Fe 3*d* electron count increases as the charge transfer energy decreases due to increased $d^5\underline{L}^1$ and $d^6\underline{L}^2$ contributions to the ground state at the expense of d^4.

[S1] M. Björck, G. Andersson, *J. Appl. Cryst.* **2007**, *40*, 1174.
[S2] J. B. MacChesney, R. C. Sherwood, J. F. Potter, *J. Chem. Phys.* **1965**, *43*, 1907.
[S3] P. M. Woodward, D. E. Cox, E. Moshopoulou, A. W. Sleight, S. Morimoto, *Phys. Rev. B* **2000**, *62*, 844.
[S4] P. C. Rogge, R. J. Green, P. Shafer, G. Fabbris, A. M. Barbour, B. M. Leffler, E. Arenholz, M. P. M. Dean, S. J. May, *Phys. Rev. B* **2018**, *98*, 201115.
[S5] M. Abbate, F. M. F. de Groot, J. C. Fuggle, A. Fujimori, O. Strebel, F. Lopez, M. Domke, G. Kaindl, G. A. Sawatzky, M. Takano, Y. Takeda, H. Eisaki, S. Uchida, *Phys. Rev. B* **1992**, *46*, 4511.
[S6] R. D. Cowan. *The Theory of Atomic Structure and Spectra*. University of California Press, Berkeley, CA **1981**.
[S7] R. J. Green, M. W. Haverkort, G. A. Sawatzky, *Phys. Rev. B* **2016**, *94*, 195127.